Bioactive Composites with Designed Interphases Based on Hyperbranched Macromers

Rodrigo L. Oréfice,[1] Arthur E. Clark,[2] Anthony. B. Brennan[3]

[1]*Department of Metallurgical and Materials Engineering, Federal University of Minas Gerais, R. Espírito Santo 35/206 –Belo Horizonte, MG, 30160–030, Brazil*
[2]*College of Dentistry, University of Florida, Gainesville, Florida 32610-0435*
[3]*Department of Materials Science and Engineering and Biomedical Engineering, University of Florida, Gainesville, Florida 32611-6400*

ABSTRACT: A series of designed interphases was produced by grafting chemically modified poly (aryl ether sulfones) (PSF) onto bioactive glass (BAG) particles. Macromolecular architecture, polymer morphology, composition and crosslink density of these PSF hybrid interphases were studied with respect to influence on mechanical properties. The hybrid PSF interphases improved mechanical strength by 20% over conventional silane treatments and increased the overall energy to failure by nearly 100%. The structure of the interphase was modeled with a three-phase viscoelastic model. The results demonstrated the ability to engineer an interphase having hyperstructures containing mobile species and inorganic functionalities that improve adhesion and favor energy release during fracture processes. © 2005 Wiley Periodicals, Inc. J Appl Polym Sci 99: 1153–1166, 2006

Key words: interface; composites; coupling agents; hybrids

INTRODUCTION

Interfacial interactions regulate the performance of many applications involving polymers. In biomedical applications, for example, natural polymers (such as proteins) interact with the surface of synthetic polymers to define the behavior of biomaterials. In these applications, chemical interactions, conformational changes, and selective adsorption are some of the critical phenomena attributed to the interfacial region. Polymers bonded to particles also influence the behavior of powder suspensions toward coagulation or deflocculation. Furthermore, in polymer composites, interfacial interactions between fibers and matrices control the overall mechanics of the material.

Just as in any bulk material, where the structure dictates properties, there is also a relationship between the structure and properties of the interfacial region. Some properties that are particularly important for the performance of interfaces in polymer systems are chemical reactivity (toward compatibilization or reaction between phases), capability of chain interpenetration, density and mechanical properties, among others. Some structural parameters that can control these properties include macromolecular chemical architecture, chain conformation, molar mass, and crosslink density (or entanglement density).

In this work, interfaces involving polymers had their structures engineered, i.e., designed and processed, to successfully fulfill their tasks as active components in a system. To alter the structure of the interface, a pure commercial polymer (PSF) was progressively and carefully modified to incorporate different chemical functionalities that would ultimately result in a range of chemical reactivities and mechanical properties. This structurally modified polymer was then inserted in an unreacted PSF as an artificial interphase to regulate the interaction of the polymer with rigid inorganic surfaces.

Controlling interfacial interactions between inorganic rigid surfaces and polymers has been one major goal in many applications[1–3] that involve polymers recently, such as adhesives, coatings, and composites. Several approaches have been taken to improve adhesion, which include plasma treatments,[4] the use of silane coupling agents,[5,6] grafting polymers onto the surface of fibers,[7,8] and the use of reactive polymers during in situ compatibilization.[9] Although these treatments can be successful in improving wetting between phases, they usually do not provide the necessary chemical and structural versatility to allow the manufacture of interfaces capable of accomplishing multiple tasks.[1]

The goal of this study was to produce hybrid interphases that could efficiently transfer stress, improve environmental stability, and enhance toughness. To accomplish this goal, novel reactive chemical groups as well as inorganic functionalities were incorporated into PSF to produce macromers that enable one to engineer mechanical and chemical behavior of the interfacial region through interactions between a PSF matrix and inorganic surfaces. These hyperstructured macromers, which contained multiple chemical functionalities, upon polymerization produced a variety of organic–inorganic hybrid structures. The complex morphologies generated are very attractive for tailoring interphases between polymers and inorganic surfaces. The hyperstructured macromers are described here in terms of interfacial properties. It is anticipated that the structure of these materials will be very useful in reinforced composites for (a) improved stress transfer, (b) enhanced adhesion and chemical compatibility, and ultimately (c) increased toughness through energy dissipation during fracture processes.

EXPERIMENTAL

Preparation of modified PSF coupling agents

A shorthand nomenclature, which is used throughout this manuscript to describe the various macromers and composite structures investigated, is defined in Table I. Homogeneous *hyper*structured polymer structures were prepared by adding special chemical functionalities to PSF. Sulfonated PSF (SPSF) was produced by attaching sulfonic acid groups to PSF. PSF (Udel®-Union Carbide) was dissolved in dichloroethane (10 wt %). Chlorosulfonic acid was subsequently added to the solution at room temperature and the resultant mixture was stirred for 30 min. Methanol was then added to the reactor vessel to force polymer precipitation. The molar ratios between chlorosulfonic acid/PSF repeat unit used was equal to 1.

Preparation of polymer–siloxane *hyper*structures

Polymer–siloxane *hyper*structures were formed within modified SPSF frameworks by inserting inorganic moieties into previously activated sites. Sulfonic acid groups on PSF were initially used as sites for the incorporation of alkoxysilane groups. Glycidoxypropyltrimethoxysilane (GPS) was added to a solution of sulfonated SPSF in dimethylformamide (DMF, 5 wt %). Films were cast on glass slides at 60°C and dried overnight at 160°C. The molar ratio GPS/SPSF repeat units used was equal to 1.

To increase the amount of siloxane bonds in SPSF frameworks, tetraethoxy silane (TEOS) was used. TEOS followed by water (water/silane molar ratio = 3) at pH = 1.5 (adjusted with HNO_3) was added to a solution of GPS-modified SPSF in dry DMF (5 wt %). Films were cast on glass slides at 60°C and dried overnight at 160°C. The final mass ratio of SPSF to silanes ratio was 1 : 1.

Preparation of polymer–siloxane *hyper*structures containing oligomers

Poly(tetramethylene oxide) (PTMO; M_w = 1000 g/mol, Polyscience), oligomers were incorporated within polymer–siloxane *hyper*structures by endcapping the hydroxy terminated-PTMO with isocyanatopropyl triethoxysilane (Polyscience). The reaction was carried at 70°C for 60 h and monitored by using FTIR.

Incorporation of PTMO oligomers within the PSF–siloxane *hyper*structures was accomplished by adding TEOS to a DMF solution of SPSP–GPS (5 wt %). HCl acidified water (pH = 1.5) was added to yield a water/silane molar ratio of 3 and stirred. After 15 min, the alkoxysilane endcapped PTMO was introduced into the mixture and continually stirred for 1 hour at room temperature in a closed Erlenmeyer flask. Films were cast on glass slides at 60°C and dried overnight at 160°C. The final composition of the solution had weight ratios of silanated SPSF/Endcapped PTMO = 2.3 and silanated SPSF/TEOS = 2.3.

Composites with silane-treated glass particles

Silane treatment on bioactive glass particles

Sodium carbonate, calcium carbonate, phosphorous and silicon oxides were melted at 1350°C to yield a bioactive glass (BAG) melt with the following composition: 46.1 mol % SiO_2, 26.9% CaO, 2.6% P_2O_5, and 24.4% Na_2O. BAG particles were produced by quenching the glass melt in water, followed by ball milling and sieving steps. The sieved glass particles, which had a size distribution between 45 and 38 μm, were treated with 2 wt % aminopropyltriethoxysilane (Aldrich) in an ethanol–water solution (95% of ethanol). Silanated particles were collected via filtration and cured for 24 h at 110°C in air.
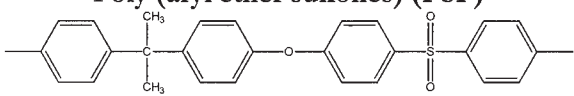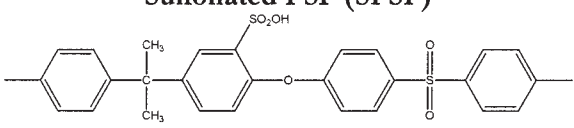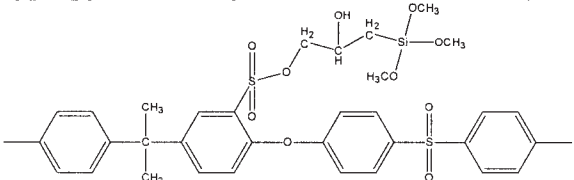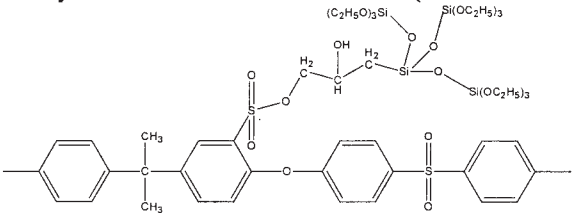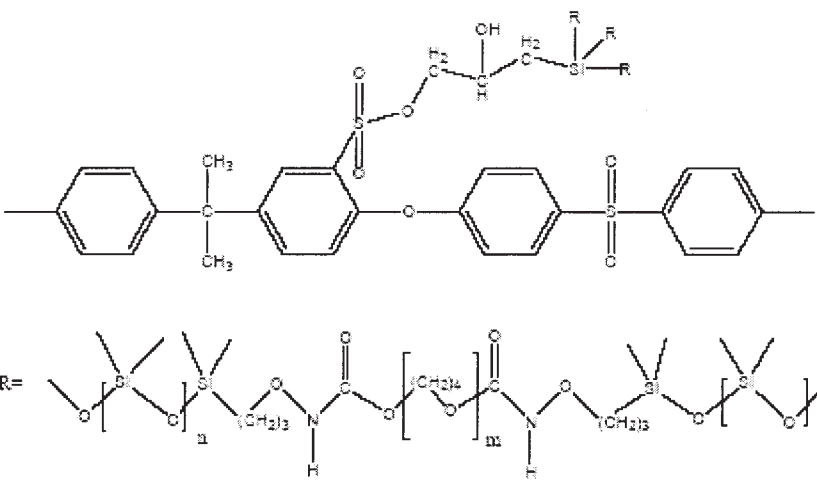
*Hyper*structured interphases grafted onto glass particles

*Hyper*structures based on PSF were grafted onto glass particles and incorporated into unmodified PSF matrices. Glass particles with natural surfaces were dispersed in a choloroform solution of the modified PSF. After 1 h, the particles were collected by filtration and washed exhaustively with the solvent. In one experiment, aminopropyltriethoxysilane-treated particles (instead of untreated BAG particles) were reacted with SPSF.

Synthesis of psf composites having *hyper*structured interphases

BAG particles with modified surfaces were mixed with unmodified PSF in chloroform (20 vol %) for 10 min at ambient conditions. The polymer/glass mix-

TABLE I
Assigned Nomenclature and Chemical Structures of Modified PSF

Poly (aryl ether sulfones) (PSF)

Sulfonated PSF (SPSF)

Glycidoxypropyltrimethoxysilane modified SPSF (GPS-SPSF)

Tetraethoxysilane modified SPSF-GPS (SPSF-GPS-TEOS)

Poly(tetramethylene oxide) (PTMO) modified SPSF-GPS-TEOS (SPSF-GPS-TEOS-PTMO)

ture was precipitated by the addition of ethanol, filtered and subsequently dried for 2 days at 90°C and 12 h in a vacuum at 160°C (30 in Hg). The mixture was then hot pressed at 205°C to form the composites. Rectangular samples were cut from the molded composite with a water-cooled diamond-saw. PSF composites having 20 vol % of untreated glass particles (45–38 μm) and composites having 20 vol % of aminopropyltriethoxysilane treated glass particles (45–38 μm) were prepared in a similar manner.

The volume fraction of particles in the composites was determined by combining picnometry (density measurements) of the samples and thermogravimetry (mass of the sample left after heating up to 900°C). The densities of the produced composite were within a 2% deviation from the theoretical density and the estimated volume fraction was then confirmed.

Methods of analysis

Mechanical test

Materials were mechanically evaluated by using a four point bending test apparatus in an Instron machine. Samples were tested with a constant 1 mm/mm cross-head speed. ASTM D790M-92 was followed during the test. Samples for the mechanical test were cut in rectangular shapes ($55 \times 7 \times 3$ mm^3) according to the ASTM standard and had their surfaces polished (using SiC 600 polishing paper). At least five samples of each composite were tested, as recommended by the ASTM standard.

TGA/DTA analysis

Thermal characterization of the materials was performed with a simultaneous thermogravimetric/differential thermal analysis instrument (TGA/DTA; Haake/Seiko) at a heating rate of 10°/min with a constant air purge of 200 mL/min. All samples (mass = 15 mg), which were previously dried at 60°C for 12 h prior to analysis in platinum crucibles, were directly compared to alumina. Prior to the analysis, the reference material and crucibles were heated to 1150°C under air. Typically the temperature range of analysis was 30–1100°C.

Dynamic mechanical spectroscopy analysis

The dynamic thermomechanical behavior of the composites was analyzed by Dynamic Mechanical Spectroscopy (DMS). A Seiko DMS110 interfaced with a Seiko SDM5600H Rheostation was used to study the thermomechanical behavior of samples in flexural mode. Frequencies used were 0.1, 0.5, 1, 5, and 10 Hz from 25 to 250°C at a heating rate of 0.75°C/min in nitrogen atmosphere.

FTIR

Infrared spectra of thin films of modified PSF were collected by transmission FTIR (Nicolet spectrometer 20SX) from 128 scans obtained with 4 cm^{-1} resolution.

X-ray photoelectron spectroscopy

X-ray photoelectron spectroscopy (XPS) was performed in a XPS system, Kratos DS800 Mg radiation. A 90° incident beam was used and the results were corrected using the carbon photoelectron peak at 285 eV. Prior to the analysis, the samples were dried at 90°C and reduced pressure for 12 h.

RESULTS AND DISCUSSION

### 3.1 Chemical structure of interphases

FTIR spectra of the *hyper*structured PSF (Fig. 1) confirm the chemical modifications of the PSF homopolymer (band assignments listed in Table II). The literature reports that the preferred site of sulfonation in polysulfone is at the ortho position of the phenyl ring in the Bisphenol A structural unit.[10] Sulfonation can be observed in the FTIR spectrum of Figure 1(b). New IR absorption bands can be seen at 3350, 2805, 2458, and 1028 cm^{-1}, which are associated with hydroxyl, S[bond]OH, and sulfonate bonds, as described in Table II. The absorption band at 1660 cm^{-1} can be related to C=C bonds at the sulfonated phenyl rings. The subsequent modifications of the PSF structure can also be monitored through the FTIR vibrational modes associated with the phenyl moiety of the Bisphenol A unit.

Glycidoxypropyl trimethoxysilane was the most efficient means of adding the alkoxy silane to the SPSF. Figure 1(c) shows that vibrations between 3200 and 3500 cm^{-1} (silanol groups) and 1090 cm^{-1} (Si—O—Si bonds) indicate the successful formation of the sulfoether linkage and the incorporation of siloxane bonds into SPSF.

The trimethoxysilane groups on the GPS-modified SPSF were reacted further in a sol–gel process with tetraethoxysilane to form hyperbranched interphases (SPSF–GPS–TEOS). The FTIR spectrum in Figure 1(d) confirms elimination of the alkoxide groups and formation of the Si—O—Si (1090 cm^{-1}) and Si—OH bonds (950 cm^{-1}) (Table II). The stoichiometry of the TEOS to SPSF–GPS was 1 to 2.3 and the H$_2$O to silane was 3 to 1.

The fourth hyperbranched structure produced was an organic/inorganic hybrid structure, based upon the polymerization of the SPSF–GPS–TEOS with a trimethoxysilane endcapped oligomer of PTMO. In Figure 1(e), the vibrational modes of the carbonyl absorption at 1715 cm^{-1} confirm the formation of the hyperbranched structures on the basis of organic–inorganic hybrids.

TGA and XPS were used to check the ability of the modified PSF to be grafted onto the surface of bioactive particles. The hyperbranched interphases produced by reaction of the BAG particles with SPSF grafts were estimated to be approximately 2% of the mass of the modified glass particles. This was based
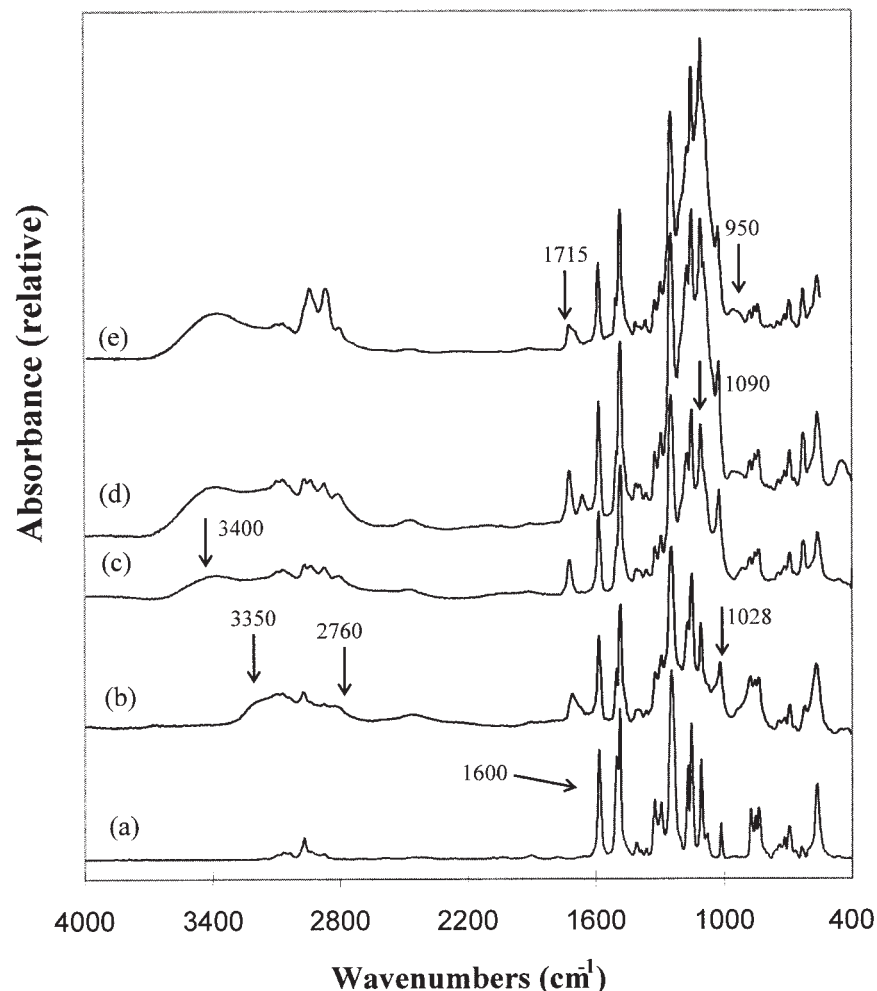
Figure 1 FTIR spectra of a series of hyperstructured PSF: (a) PSF; (b) hyperstructured PSF with sulfonic acid groups (SPSF); (c) PSF–siloxane hyperstructures derived from GPS (SPSF-GPS); (d) PSF–siloxane hyperstructures derived from GPS and TEOS (SPSF–GPS–TEOS); (e) PSF–siloxane hyperstructures containing PTMO (SPSF–GPS–TEOS–PTMO). Arrows mark some of the most important absorption bands.

upon weight losses measured by TGA in a nitrogen atmosphere. An initial weight loss of 2% that begins at ambient and continues to about 200°C was attributed to physical adsorbed and chemically bound water as well as residual solvent (Fig. 2). The second mass loss of another 2% that begins at 450°C was assigned to the decomposition of the grafted SPSF polymer. Similar behavior was also observed for the glass particles coreacted with the other *hyper*structured PSF.

Further evidence of the chemical structure of the hyperbranched interphases bonded to the BAG was provided by XPS. The XPS spectrum (from 0 to 600 eV) of a BAG substrate in Figure 3(b) shows the presence of Ca, Si, O, and P on the surface of the glass, as it would be predictable, since these elements are the main components of the BAG. In Figure 3(a), the XPS spectrum of a BAG coated with APS and subsequently reacted with the SPSF illus-

trates the presence of mainly C (1s), S (2p), and O (1s) structures, which confirms the presence of the sulfonated polymer on the surface of the glass. The theoretical composition of the SPSF was calculated using the values of degree of substitution (1.0) for the *hyper*structured polymer used in this work. These calculations (shown in Table III) were performed by simply computing the percent of each element in the structural formula of SPSF. The theoretical composition was then compared with the measured one, which was obtained by integrating the area under each XPS peak. The small difference between measured and theoretical compositions demonstrated that a large part of the surface of the glass substrate was covered with the *hyper*structured SPSF. Moreover, the new polymer was grafted on the surface of glass possibly through covalent bonds between sulfonic acid group and amine groups on the silane layer (formation of sulfonamide bonds —SO_2—NH—).

TABLE II
FTIR Absorption Peaks in Modified PSF: Experimental and Guidelines for Indentification

|	Observed peaks (cm^{-1})	Peak assignment
PSF	3050–3000	C—H stretch in aromatic rings
	2950–2750	CH, CH2, CH3 stretch
	1600–1500	C=C stretch in aromatic rings
	1376–1300	C—SO$_2$—C groups
	1250	C—O stretch on the Bisphenol A unit
	1100–1000	S=O
	740–690	C—S stretch
SPSF	3350	3600–3200 cm^{-1}: OH groups
	2805 and 2458	2800–2200 cm^{-1}: SOH
	1028	1080–1000 cm^{-1} symmetric stretching of the sulfonate group
SPSF–GPS	3500–3200	Silanol groups (SiOH)
	1100–900	Siloxane bonds
SPSF–GPS–TEOS	3500–3200	Silanol groups
	1100–1000	Sioxane bonds
	980–900	Silanol bonds
SPSF–GPS–TEOS–PTMO	3500–3200	Silanol and glycol groups
	1100	C—O—C (PTMO)
	1715	Carbonyl
	1100–900	Sioxane bonds
	3325 and 1560	Secondary amine

Mechanical properties of SPSF macromers in BAG composites

Engineered interphases SPSF in BAG composites

Table IV reports the results of mechanical tests performed in composites having different interphases. The average value together with the standard deviation of each evaluated mechanical property was used in this work to indicate evidences of differences in mechanical properties among the different materials. Table IV shows that the elastic modulus of composites with *hyper*structured interphases as well as with silane treated particles was improved markedly when compared with composites with untreated particles. The silane treatment led also to an improvement in the strength of the composites, but the largest improvements were obtained by constructing interphases based on *hyper*structured polymers. It is important to emphasize that the yield strength of PSF is around 107 MPa, and values close to this number were obtained in particulate composite with a *hyper*structured interphase based on PSF with sulfonic acid units. The silane treatment on particles can produce high interfacial strength and also rigid interfaces, leading to high levels of stress transfer and composites with enhanced modulus. Rigid interfaces, although increasing the energy for debonding, cannot dissipate the energy of cracks.[1] Thus, any crack that is nucleated can propagate with less energy relief. Otherwise, a *hyper*structured interphase can help dissipating the energy for crack propagation.

The stress–strain curves in Figure 4 also reveal that the silane treated particulate composites have low strain at failure values. Although, fracture toughness was not measured in this work, the concept of the total energy to failure (represented by the area under the stress–strain curve) was used to provide information about toughness (Table IV). Thus, the composite with silane-treated particles behaves in a more brittle manner than the other composites (according to the total energy of failure). This can be, again, explained by the formation of rigid interfaces that do not have mechanisms of energy relief at crack tips. Cracks can then propagate fast throughout the material.

On the other hand, larger values of strain at failure were observed for untreated particulate composites. In this case, the presence of voids at poor-bonded interfaces can increase the radius of the crack tip, increasing the energy for their propagation and expanding the strain at failure. Larger values of elongation to failure were also noted for particulate composites with a *hyper*structured interphase, based on PSF with sulfonic acid. The energy to failure was also much higher for this composite, and high levels of toughness can be predicted for this material. Therefore, it was observed that the use of a silane treatment alone could not improve strain to failure due to the formation of a stiff and strong interface. On the other hand, the combination of a silane treatment and SPSF provided synergy, resulting in improvement of both strength and strain to failure.
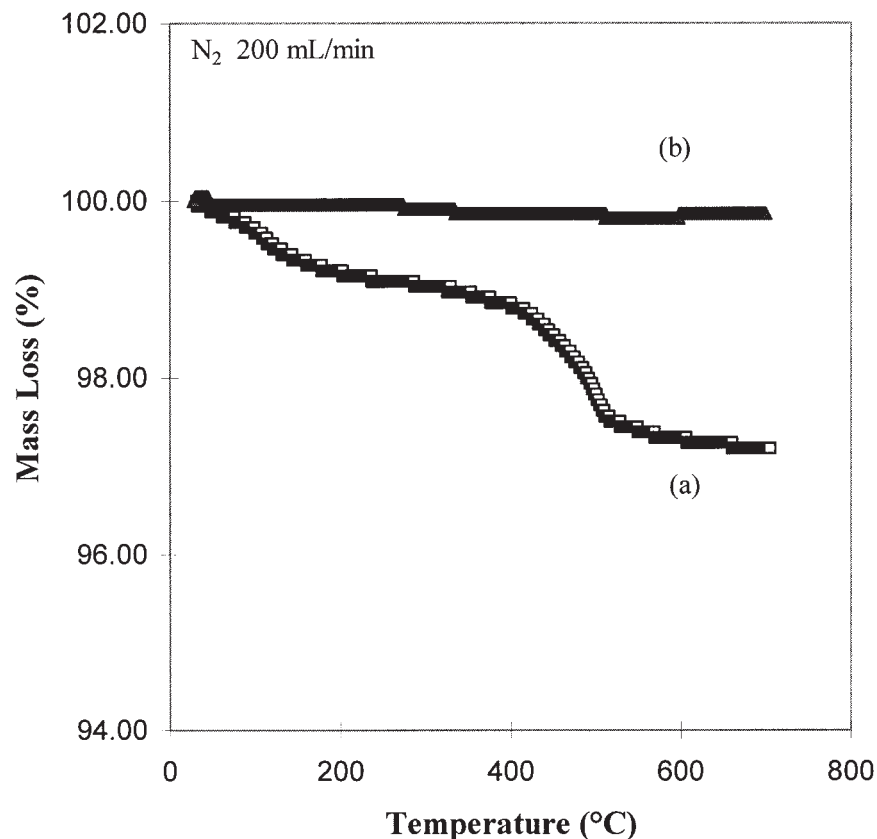
Figure 2 Thermogravimetric analysis (TGA) on (a) *hyper*structured PSF with sulfonic acid groups grafted on BAG particles and (b) aminopropytriethoxysilane-treated BAG particles.

Thus, mechanical tests showed that composites with a *hyper*structured interphase, based on PSF with sulfonic acid units, led to the production of composites with high elastic modulus, high strength, and high energy to failure (an indication of high toughness). From XPS studies, it was demonstrated that sulfonic acid groups could bond to inorganic surfaces via sulfonamide bond formation. In *hyper*structured interphases, formation of bonds between polymers and surface groups can be carefully designed to yield the desired result. The attachment of sulfonic groups into PSF to produce a *hyper*structured interphase was planned to favor the formation of few linkages between the polymer and the rigid surface, thus allowing the presence of fairly large nonbonded chain lengths. In PSF with sulfonic acid units (low degrees of substitution), polar groups (sulfonic acid) are followed by long hydrophobic units (aryl groups). This chain configuration is thought to induce interactions between polar groups of the macromer and the surface bound polar groups, i.e., amines and silanols, and facilitate interaction between hydrophobic units of the SPSF polymer backbone and the bulk PSF. The morphology of this hyperstructured interphase would then be comprised of a distribution of lengths (or loops) of nonbonded chain fractions entangled with each other.[11]

It is proposed that this hyperstructured interphase with the distribution of chain fractions can also create a range of entanglement densities that facilitate interpenetration of chains by the PSF matrix. Higher levels of chain interdiffusion can lead to a higher magnitude of intersegmental bonding and entanglements between chains at the interphase and chains from the matrix. Entanglements between the grafts and the polymeric matrix coupled with short range bonding (i.e., van der Waals, polar, and hydrogen bonding) could then increase the stress transfer function, which equates to improved toughness.

Engineered interphases of SPSF–GPS–TEOS in BAG composites

SPSF–siloxane hyperstructured interphases substantially improved the mechanical properties of the composites (Table IV, Fig. 4). The elastic modulus increased significantly along with the strength and strain at failure for composites with the SPSF–siloxane hyperstructured interphases. As previously stated, large values of elastic modulus were also obtained for composites with particles treated only with a silane agent; however, low values of energy to failure were also observed.
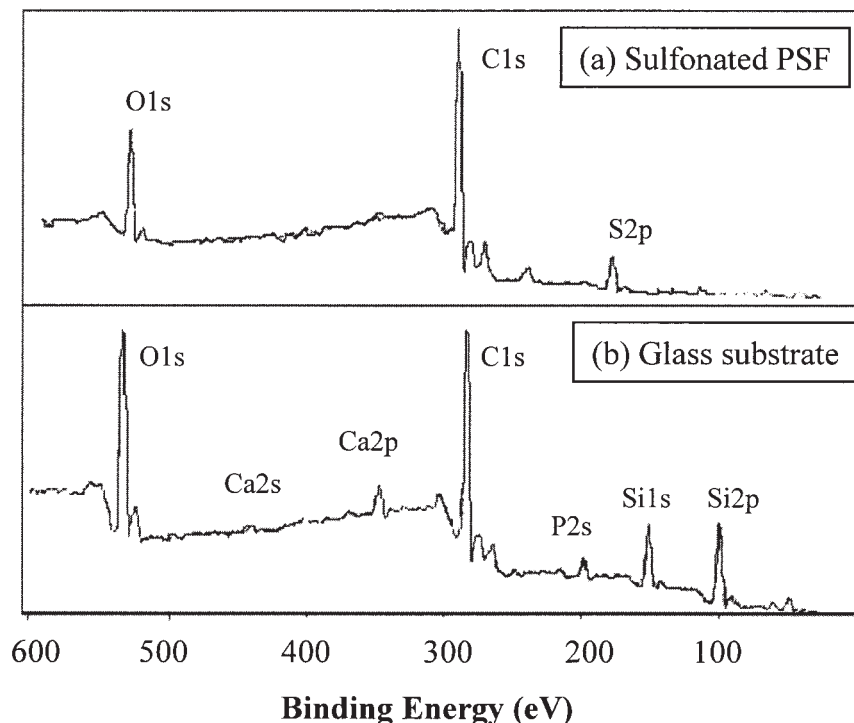
Figure 3 XPS spectra of pure BAG disk (b) and BAG disk with grafted PSF macromers (a).

Mechanical properties of composites having interphases with different contents of siloxane bonds (i.e., silanated SPSF derived from GPS versus SPSF–siloxane *hyper*structures derived from GPS and TEOS) were very similar. The similarity in results was probably a consequence of the large inorganic content of the silanated SPSF. For these materials (used as interfacial agents), the improvement in properties was based on the enhanced interaction between phases and formation of an interphase with graded elastic modulus that will favor stress transferability by reducing the abruptness of the interface. Natural polymer–inorganic interfaces have a discontinuity in mechanical properties, particularly in terms of stiffness (elastic modulus). It is proposed here that stress transferability at the interface can be improved by breaking the discontinuity of properties in this region through the creation of a *hyper*structured interphase. Siloxane groups on *hyper*structured polymers improve the modulus of the original polymer by introducing strong ceramic type of bonds (Si—O—Si bonds present in the modified PSF interfacial agent) and by forming crosslinks between polymer chains.[12,13] Figure 5 shows a schematic diagram revealing the structure of the interphase containing a modified PSF when compared with a more conventional silane treated interface. Figure 5 also exhibits the proposed idea of the formation of an interphase with graded elastic modulus (*E*).

Engineered interphases SPSF–GPS–TEOS–PTMO in BAG composites

The last hyperstructured interphase tested was based on polymer–siloxane networks containing PTMO oligomers. The results of the mechanical test (Table IV) showed evidences that the elastic modulus may have been reduced because of the introduction of low T_g chains at the interphase. Basically, stress transferability is reduced because partial stresses are consumed on relaxation phenomena of the high mobile chains. On the other hand, the total energy of failure was improved as a possible indication that the PTMO low-T_g chains were contributing in the overall mechanism of energy dissipation during crack propagation. High mobile chains can

TABLE III
Comparison between XPS Theoretical and Measured composition—BAG Grafted with PSF Macromers

Elements	PSF[a] (wt %)	SPSF[a] (wt %)	SPSF grafted onto BAG (wt %)
C (1s)	77.1	62	61.67
O (1s)	15.3	24	23.13
S (2p)	7.6	14	13.34
N (1s)	—	—	—
Ca (2p)	—	—	1.82
Si (2p)	—	—	—
P (2p)	—	—	—

[a] Theoretical values.

TABLE IV
Mechanical Properties of Poly (aryl ether sulfones)-20 vol % BAG Composites with PSF Macromers
as Interfactal Agents

Hyperstructured interphase	Elastic modulus (GPa)	Strength (MPa)	Strain (%)	Energy[a] to failure (J/m^3)
PSF/BAG	4.6 ± 0.14	83 ± 3.1	2.5 ± 0.2	1.04 ± 0.05
PSF/BAG–APS	5.2 ± 0.16	88 ± 2.3	1.9 ± 0.1	0.84 ± 0.05
SPSF/BAG–APS	5.1 ± 0.15	105 ± 3.7	2.9 ± 0.1	1.52 ± 0.09
SPSF–GPS/BAG	5.2 ± 0.16	94 ± 2.1	2.5 ± 0.1	1.18 ± 0.06
SPSF–GPS–TEOS/BAG	5.4 ± 0.16	96 ± 2.0	2.6 ± 0.1	1.25 ± 0.06
SPSF–GPS–TEOS–PTMO/BAG	4.9 ± 0.15	97 ± 1.9	2.8 ± 0.1	1.36 ± 0.06

[a] Total energy to failure = area under the stress-strain curve.

undergo conformational transitions when submitted to stresses and therefore can consume the energy associated with the process. This type of hyperstructured interphase, more than able to dissipate energy (and therefore improve toughness of the composite), can also work as self repair device, since no permanent damage is introduced to the interface during the energy dissipation process through conformational changes.

Morphological features of composites with designed interphases

The morphology of the fractured surface of composites having *hyper*structured interphases was also investigated to reveal mechanisms of fracture and adhesion. The fractured surface of a PSF-20 vol % glass composite with untreated interfaces contained voids related to particle deboding and pull-out during frac-
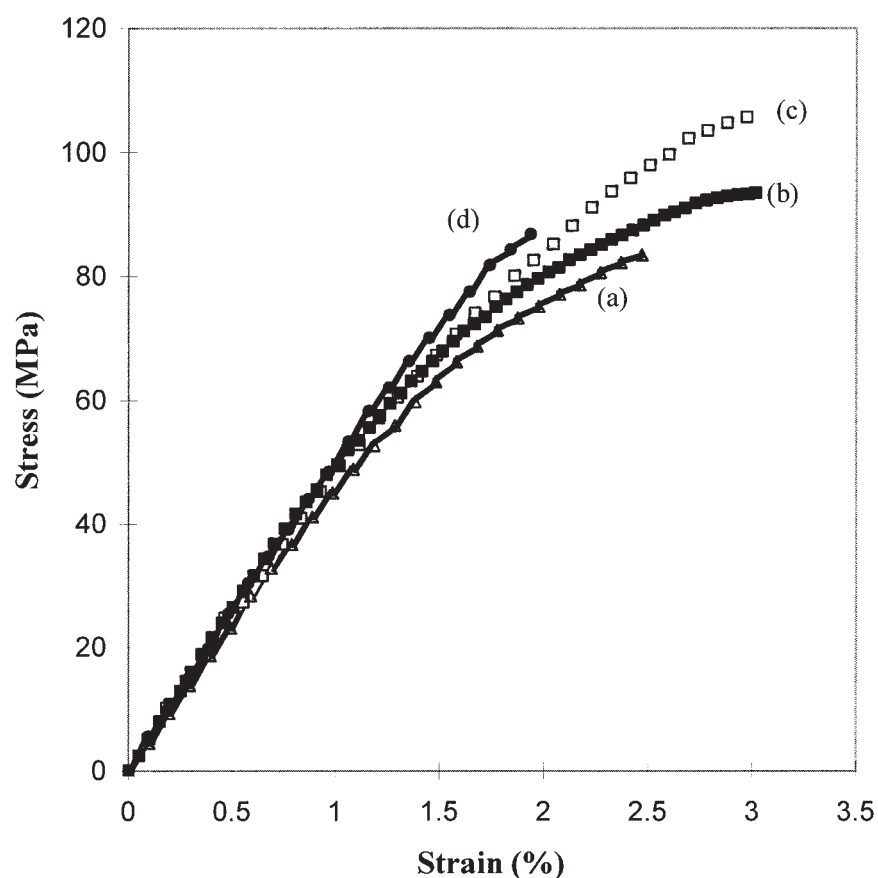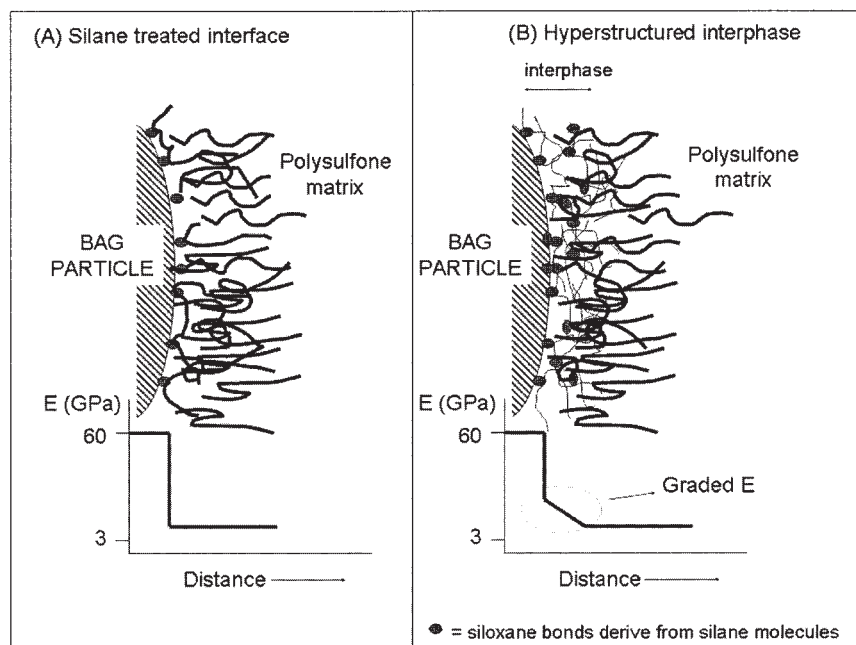

Figure 4 Stress–strain curves for PSF–BAG composites having different interphases: (a) untreated interfaces; (b) *hyper*structured SPSF–GPS–TEOS; (c) SPSF grafted onto aminopropyltriethoxysilate-treated BAG particles; (d) silane-treated BAG particles.

Figure 5 Schematic representation of the interphase containing modified PSF compared with a more conventional silane-treated interface (E = elastic modulus).

ture [Fig. 6(a)]. There was no detectable polymer on the exposed particles. On the other hand, a polymeric film partially covering the exposed particles is apparent on the fractured surface of composites having a *hyper*structured interphase composed of SPSF [Fig. 6(b)]. Hence, a high level of interfacial adhesion was achieved when compared with the composite with untreated interfaces.

## DMS on composites having designed interphases

The dynamic elastic modulus of composites that were either treated with silane or composed of a hyperstructured interphase, based on PSF with sulfonic acid groups, were higher than those with untreated particles (Fig. 7, Table V).

No major changes on the α-relaxation (i.e., T_g) of the composites were detected (Table V). On the other hand, the activation energy (calculated using DMS results) for the α-transition increased from untreated composites to treated ones. The largest increase in activation energy was obtained for composites having hyperstructured interphases, based on SPSF. From the results of activation energy, it is possible to say that the creation of hyperstructured interphases interfered with the processes related to the glass transition by reducing the mobility of the chains close to rigid surfaces. Entanglements between chains from the matrix and chains attached to a surface can reduce the mobility of chains more than entanglements between free chains in bulk.

The effect of different interphases on the thermomechanical behavior of composites can be seen easier when the loss tangent at the γ-relaxation is studied (Table V). The usual trend of increasing the temperature of the transition and reduction of the loss tangent values due to the presence of rigid interphases can be observed when composites with untreated interfaces are compared with silane treated interfaces and with composites with hyperstructured SPSF interphases. As reported in Table V, the magnitude of the loss tangent for the sub-T_g was lower and the activation energy was higher for composites with engineered interphases in comparison with composites with untreated glass particles. Therefore, there is an indication that the short-range movements of chains (ring rotation, etc.) at low temperatures were much more affected by the interfacial interactions than long-range movements at higher temperatures for the system of this work.

To get more information about the effect of the engineered interphases on the relaxation processes of the system, a physical model was applied to the data. This model relates the dynamic (complex) elastic modulus to the unrelaxed, relaxed modulus and relaxation times and uses parameters from the Cole–Cole plot to fit the experimental data to the model,[14,15] as indicated in eq. (1).

A Cole–Cole type of plot was first developed for studying dielectric phenomena, but is also applied to viscoelastic phenomena, since this approach also has an intrinsic time–energy relationship. Relaxation pro-
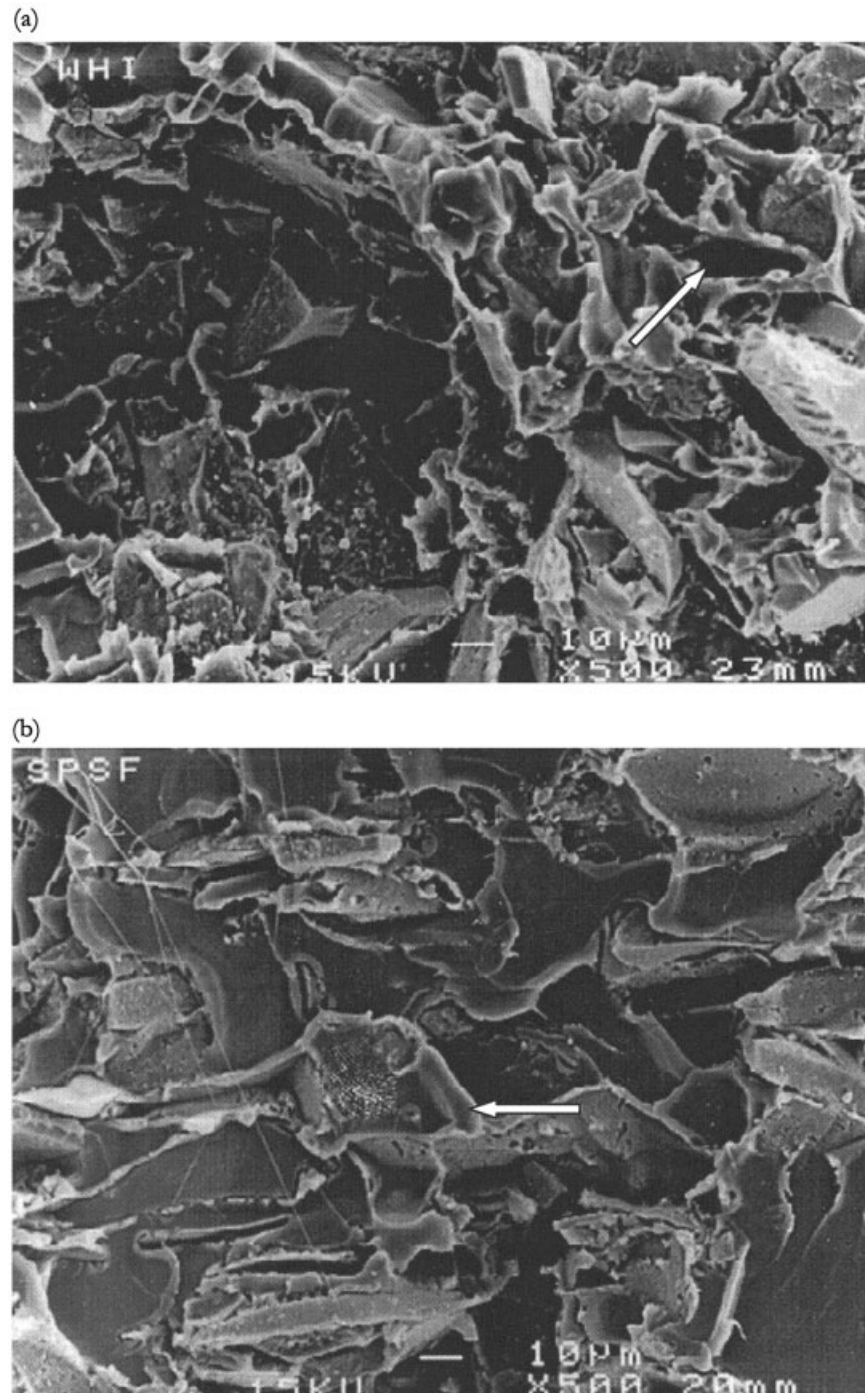
Figure 6 SEM micrographs of the fractured surfaces of PSF-20 vol.% BAG composites with untreated interfaces (a) and hyperstructured interphases based on PSF macromers (b). Arrows reveal voids in untreated interfaces (a) and particles covered with polymer in treated interfaces (b).

cesses during viscoelastic transitions are well emphasized by Cole–Cole plots. These relaxation processes are seldom represented by only a single relaxation time and a distribution of relaxation times might be required to express the whole process occurring in a common polymer. The complexity of the relaxation phenomenon can be attributed to factors such as differences in chemistry and structure of segmental units within a polymer repeat unit, different environments for the chains, inhomogeneities due to inherent processing deficiencies (molar mass distribution, free volume distribution, etc.), and thermomechanical history. When rigid surfaces are in contact with polymers, the mobility of the chains is constrained by both the physical presence of the surfaces and any possible chemical interaction between the phases. Moreover, the relax-
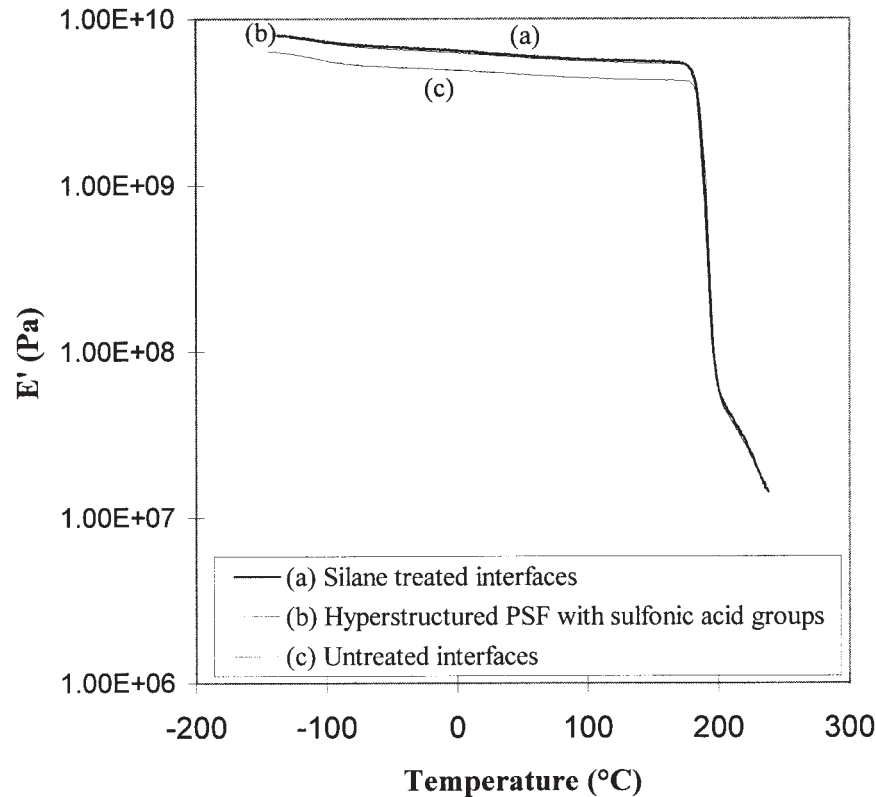
Figure 7 DMS storage elastic modulus (1 Hz) of PSF-20 vol % BAG composites with different interphases.

ation processes of polymeric chains near rigid surfaces are often modified by changes in mobility as well as conformational structure of the chains. In this situation, relaxation processes are enthalpically and entropically modified, since different levels of energy are required for transitions to occur and new conformational modes are imposed to the chains. The magnitude of the changes in the relaxation phenomena due to the presence of the interface is related to the degree of interaction between phases of the composite. When lack of wetting and therefore poor adhesion between the phases is present, the relaxation processes will be less affected. Otherwise, when strong interfacial bonds can occur across the interface, a thicker interphase will be formed and its effect will be more pronounced on the relaxation processes.

$$E^* = E_r + \frac{E_u - E_r}{1 + (iw\tau_1)^{-h} + (iw\tau_2)^{-k}} \qquad (1)$$

where E^* is complex modulus; E_r, relaxed modulus; E_u, instantaneous modulus; τ_1 and τ_2, relaxation times; w, frequency, h, long time parameter; and k, short time parameter.

Values for the relaxed and unrelaxed modulus can be obtained from a Cole–Cole plot by extrapolating the data to near zero loss ($E'' = 0$). Parameters h and k are used to fit the model to the data. They are usually obtained from a experimental Cole–Cole plot, where the storage modulus is plotted against the loss modulus. Both parameters can be calculated from angles in which the curves reach the E' axis of the Cole–Cole plot: $h = 2\theta_r/\pi$ and $k = 2\theta_u/\pi$, where h is the long time

TABLE V
DMS Results of PSF Composites with 20 vol % of BAG

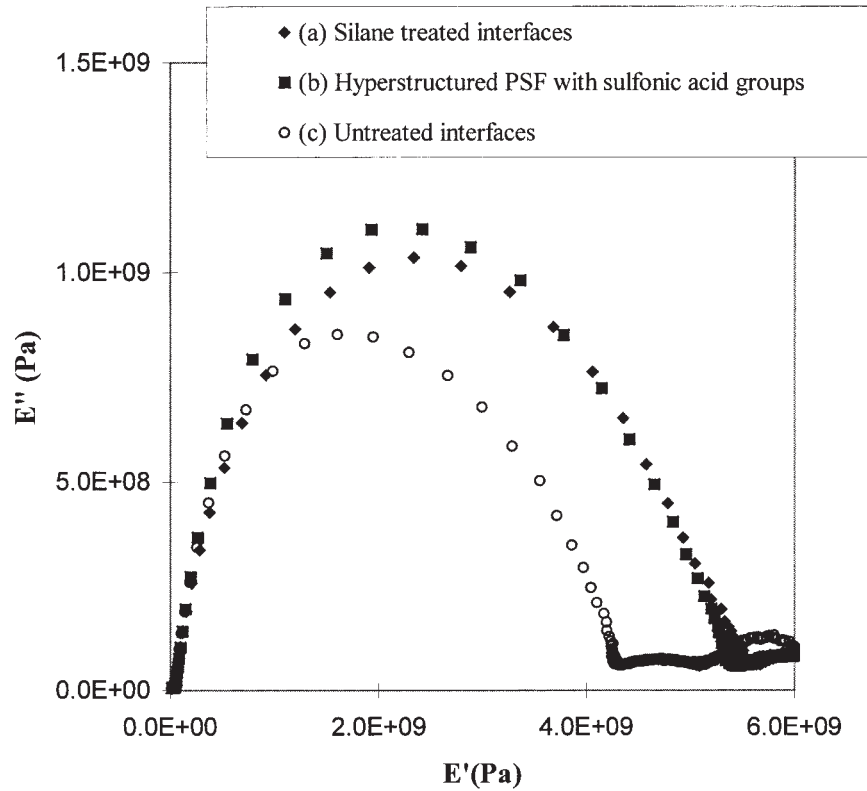|	Untreated interfaces	Silanated interfaces	SPSF
E' (GPa): 1 Hz at 25°C	4.8	6.2	6.0
T_g (°C)	194°C	193.7°C	193.4°C
Loss tangent at T_g	1.4	1.3	1.4
Activation energy (kJ/mol) of T_g	896.2	910.4	928.5
sub-T_g transition (°C)	−106.7°C	−102.5°C	−102.0°C
Loss tangent at sub-T_g	0.022	0.018	0.018
Activation energy (kJ/mol) - Sub T_g	38.7	44.0	48.2

Figure 8 Cole–Cole plot (1 Hz) of PSF-20 vol % BAG composites with different interphases.

parameter and k is the short time parameter. Both h and k parameters can be related to inhomogeneities within the material, which would disturb the relaxation processes. Thus, lower values for h and k can represent a less Gaussian distribution of relaxation times with more pronounced tails. In terms of a composite, the interface is a type of inhomogeneity that can lower the values of k and h by interfering in the relaxation phenomena of chains nearby.

The Cole–Cole type of plot (1 Hz) for three composites with different interphases illustrates that the structure of this region altered the phenomena associated with chain mobility and relaxation (Fig. 8). Parameters h and k were used to fit the model to the data. The values of k, h, and unrelaxed and relaxed modulus for the composites are displayed in Table VI. Reduction in

the values of h and k (mainly in k) for *hyper*structured interphases demonstrated that these modifications introduce constraints by reducing the chain mobility at interface. Higher levels of interfacial adhesion due to intersegment interactions and chain entanglements on composites with *hyper*structured interphases can be responsible for the imposed constraints on chain mobility. This result supports earlier discussions regarding the effect of *hyper*structured interphases on the total energy of failure of composites.

CONCLUSIONS

In this work, a series of hyperstructured interphases was engineered and applied to rigid surfaces in con-

TABLE VI
Physical Modeling of Interfaces Using Cole–Cole Type of Plot: PSF-20 Vol % Glass Composites
with Hypersturctured Interphases

Type of interfacial modification	Relaxed elastic modulus (MPa)	Unrelaxed elastic modulus (GPa)	h	k
Pure PSF (no rigid surfaces)	60	2.7	0.722	0.9
Unmodified interfaces	40	4.35	0.74	0.59
Silane treated interfaces	45	7	0.69	0.29
*Hyper*structured PSF with sulfonic acid groups	48	5	0.705	0.382

tact with polymers. The effect of several structural parameters of these synthetic hyperstructured interphases on the behavior of the systems regarding stress transferability, chain interpenetration, adhesion and chain relaxation, was investigated.

It was shown that stress transferability (elastic modulus and strength) and toughness can be improved by creating hyperstructured interphases capable of bonding to rigid surfaces as well as suitable to promote interpenetration of polymer chains from the matrix. Interpenetration was allowed by building interphases containing low packed polymer chains. Chain interdiffusion led to the formation of entanglements and maximization of intersegment bonding contributed to the enhancement of adhesion and toughness.

*Hyper*structured interphases having values of mechanical properties in between the properties of pure polymers and inorganic materials were fabricated by inserting siloxane bonds within a polymer framework containing reactive species. This type of interphase was able to produce composites with high elastic modulus and also toughness. In this case, it was proven that stress transferability and mechanisms of energy relief could be promoted by reducing the sharpness of natural interfaces.

References

1. DiBenedetto, T. Materials Sci and Eng 2001, A302, 74.
2. White, S. R.; Sottos, N. R.; Geubelle, P. H.; Moore, J. S.; Kessler, M. R.; Sriram, S. R.; Brown, E. N.; Viswanathan, S. Nature 2001, 409, 794.
3. Jang-Kyo, K.; Mai, Y. W. Engineered Interfaces in Fiber Reinforced Composites, 1st Ed.; Pergamon Press: Amsterdam; 1998.
4. Montes-Morán, M. A.; Martínez-Alonso, A.; Tascón, J. M. D.; Young, R. J. Composites: Part A 2001, 32, 361.
5. Suzuki, N.; Ishida, H. Macromol Sym 1996, 108, 19.
6. Kim, J. K.; Sham, M. L.; Wu, J. Composites: Part A 2001, 32, 607.
7. Lin, R.; Wang, H.; Kalika, D. S.; Penn, L. S. J Adhes Sci Technol 1996, 10, 327.
8. Arnold, J. J.; Zamora, M. P.; Brennan, A. B. Polym Compos 1996, 17, 332.
9. Shi, D.; Yang, J.; Yao, Z.; Wang, Y.; Huang, H.; Jing, W.; Yin, J.; Costa, G. Polymer 2001, 42, 5549.
10. Chen, M.; Chiao, T.; Tseng, T. J. Appl Polym Sci 1996, 6, 1205.
11. Oréfice, R. L.; Brennan, A. B. Materials Research 1998, 1, 19.
12. Ni, H.; Simonsick, W. J., Jr.; Skaja, A. D.; Williams, J. P.; Soucek, M. D. Prog Org Coat 2000, 38, 97.
13. Wen, J. Y.; Wilkes, G. L. Chem Mat 1996, 8, 1667.
14. Bergeret, A.; Agbossou, A.; Alberole, N.; Cassagnau, P.; Sarraf, T. Eur Polym Mater 1992, 28, 1201.
15. Bergeret, A.; Alberole, N. Polymer 1996, 37, 2759.